Cell Communication and Signaling

RESEARCH

Open Access

Transcription factor XBP1s promotes endometritis-induced epithelial-mesenchymal transition by targeting MAP3K2, a key gene in the MAPK/ERK pathway

Kangkang Gao[1,2], Mengqi Si[1,2], Xinxi Qin[1,2], Beibei Zhang[1,2], Zongjie Wang[1,2], Pengfei Lin[1,2], Huatao Chen[1,2], Aihua Wang[2,3] and Yaping Jin[1,2*]

Abstract

The epithelial-mesenchymal transition (EMT) is a biological process whereby epithelial cells are transformed into cells with a mesenchymal phenotype. The transcription factor, X-box binding protein 1 splicing variant (XBP1s) is a key regulator of the endoplasmic reticulum stress response (ERS); but the function of XBP1s in the endometritis-induced EMT process remains unclear. Here we found that uterine tissues from goats with endometritis exhibited an EMT phenotype, with a significant decrease in the epithelial cell polarity marker E-cadherin and a significant increase in the mesenchymal markers N-cadherin and vimentin. We also found that sustained LPS treatment induced EMT in goat endometrial epithelial cells (gEECs), along with ERS and XBP1s overexpression. *XBP1s* KO significantly inhibited LPS-induced EMT and migration in gEECs, while *XBP1s* overexpression showed the opposite result. CUT & Tag experiments performed on *XBP1s* revealed that *MAP3K2* was a downstream target gene for XBP1s regulation. We also found that expression of *MAP3K2* was positively correlated with *XBP1s* expression in uterine tissues of goats with endometritis and in gEECs. Assays for dual luciferase reporter and molecular docking indicated that XBP1s protein regulated the transcription of *MAP3K2* by modulating promoter activity. The knockdown of *MAP3K2* expression significantly inhibited the migration and EMT of gEECs. XBP1s and MAP3K2 significantly promoted phosphorylation of p38 and ERK, activating the MAPK/ERK pathway. Treatment with the MAPK/ERK inhibitor, PD98059, reversed the effects of *XBP1s* and *MAP3K2* overexpression on LPS-induced EMT. The MAPK/ERK activator, DHC, reversed the effects of *XBP1s* KO and *MAP3K2* KD on EMT.

Keywords XBP1s, Epithelial-mesenchymal transition, Endoplasmic reticulum stress, *CUT & Tag*, Molecular docking, MAPK/ERK pathway

*Correspondence:
Yaping Jin
yapingjin@163.com
Full list of author information is available at the end of the article

Introduction

Bacterial infection and tissue damage in the ruminant uterus after parturition are the major causes of endometritis, which results in huge economic losses to the livestock industry [1, 2]. Endometrial epithelial cells (EECs) play a major role in the immunoregulation of the uterus, mainly as a physical barrier against invasion by pathogenic bacteria, but also for the expression of secreted immune-associated proteins, which play a key role in triggering the innate immune response for defense against inflammatory disease [3, 4]. Therefore, a deeper understanding of the function of EECs is essential for prevention and treatment of uterine diseases in ruminants. Most ruminant endometritis is characterized by chronic inflammation or chronic inflammation that develops from acute inflammation [5]. Ruminant endometritis resulting from infection of the uterus by gram-negative bacteria such as *E. coli* is usually mediated by lipopolysaccharide (LPS) [6]. LPS is recognized by Toll-like receptor 4 (TLR4) expressed on the EEC surface. This triggers a signal transduction cascade, which induces secretion of the inflammatory mediators, IL-6 and TNF-α, causing endometrial inflammation [7].

The epithelial-mesenchymal transition (EMT) is the biological process by which epithelial cells are transformed by a specific program into cells with mesenchymal phenotype, which is one of the major ways the body responds to inflammation [8]. During the EMT, well-polarized epithelial cells lose polarity and stable intercellular junctions and acquire a spindle-shaped mesenchymal-like morphology with enhanced motility and migratory ability [9]. Numerous studies suggest that the EMT plays a critical role in embryonic implantation, tissue repair, cancer metastasis, and fibrotic diseases [10, 11]. As one of the main means for the organism to cope with inflammation, the EMT is involved in the development of various conditions such as lung inflammation and fibrosis, which is ameliorated by inhibition of the NF-κB/NLRP3-mediated EMT [12]. The EMT was also found to be induced in epithelial cells by LPS and blocking activation of the NF-κB pathway in LPS-induced acute lung injury reversed the LPS-induced EMT [13]. However, the role and mechanism of the EMT in EECs in ruminant endometritis remain poorly understood.

Previous studies have revealed that endoplasmic reticulum stress (ERS) participates in various physiological and pathological processes through activation of the unfolded protein response (UPR). The three branches of the UPR are initiated by different ERS sensors: inositol-requiring enzyme 1 (IRE1), PKR-like ER kinase (PERK), and activating transcription factor 6 (ATF6) [14]. The best conserved of these branches involves the interplay between IRE1α and XBP1s, in which ER membrane-anchored kinase IRE1α activates the transcription factor XBP1s which in turn acts as effector of the adaptive UPR. Recent studies have demonstrated the involvement of ERS in the EMT and have shown that inhibition of ERS improved EMT in renal tubular epithelial cells [15]. This suggests that ERS may also be involved in LPS-induced EMT in gEECs, although the molecular mechanisms involved remain unclear.

XBP1s is an effector of ERS. When ERS occurs, IRE1α dissociates from the ER chaperone, glucose-regulated protein 78 (GRP78), which acquires kinase and endoribonuclease activities through homodimerization and autophosphorylation [16]. This endoribonuclease activity results in unconventional splicing of unspliced XBP1 mRNA into spliced XBP1 (XBP1s) RNA by removing a 26 bp introns, and the spliced mRNA is then translated into the transcription factor, XBP1s, which matures into an active form [17]. In pronounced contrast to PERK, XBP1s protects neuronal cells from damage by inhibiting inflammation and oxidative stress [18]. XBP1s plays an important role in the development of renal diseases such as nephritis and sepsis [19] and in ER expansion, development of highly secretory cells such as plasma cells and pancreatic and salivary gland epithelial cells, adaptation of tumor cells to hypoxic conditions, and glucose deprivation [20–22]. However, the specific mechanism of XBP1s in endometritis-induced EMT remains elusive. To address this, we evaluated the EMT in goat endometritis and explored the role of XBP1s and the mechanisms involved. These results suggest that XBP1s could be a target for correcting the problem of poor reproduction and high culling rates in livestock farming.

Materials and methods

Tissue collection

Adult Guanzhong dairy goats (n = 11, aged 2–3 years, mean weight = 62.17 ± 2.01 kg) were housed and fed at the Laboratory Animal Center of Northwest Agriculture and Forestry University in Yangling, China. Normal uterine tissues were surgically removed from five healthy goats and endometritic tissues from six goats with endometritis. Part of the normal and endometritic tissues were immediately frozen in liquid nitrogen, while the rest were fixed in 4% (v/v) paraformaldehyde in phosphate-buffered saline (PBS) without Ca^{2+}/Mg^{2+}.

Cell culture and drug treatment

The gEECs were immortalized by transfection with human telomerase reverse transcriptase (hTERT), which was identified and well conserved in our laboratory [23]. HEK293T cells were obtained from the cell bank of the Typical Culture Preservation Center of the Chinese Academy of Sciences (Shanghai, China). The gEECs and

HEK293T cells were cultured in DMEM/F12 (DF12) and high glucose DMEM medium, respectively, containing 10% fetal bovine serum (FBS; Gibco, Thermo Fisher Scientific, Waltham, MA, USA) and 1% antibiotic–antimycotic (AA, containing penicillin, streptomycin, and amphotericin B; Invitrogen, Inc. Carlsbad, CA, USA) at 37°C in a humidified incubator containing 5% CO_2. When cell confluence reached 70–80%, the medium was replaced with fresh medium and the following treatments were performed: (1) LPS (5 μg/mL, Sigma-Aldrich, St. Louis, MO, USA) for 3, 6, 12, and 24 h, (2) DHC (1 μM, MAPK/ERK activator, TargetMol, Boston, MA, USA), and (3) PD98059 (10 μM, MAPK/ERK inhibitor, TargetMol). Cells were pretreated for 2 h, followed by the addition of LPS and sustained treatment at 37°C for 24 h [24].

Construction of goat XBP1s knockout (KO) cell lines

The pSpCas9(BB)-2A-GFP (PX458) vector was from our own laboratory stock. An online tool (http://chopchop.cbu.uib.no/) was used to design a high-scoring goat *XBP1s* KO site. The primer sequences are shown in Table 1. After annealing, the primer sequences were cloned into pSpCas9(BB)-2A-GFP(PX458) and transfected into gEECs. After puromycin screening, monoclonal cells were picked, sequenced, and XBP1s protein level was measured by western blotting.

Plasmid construction

The pcDNA3.1 empty plasmid came from our laboratory stock [25]. The *XBP1s* and *MAP3K2* sequences were amplified from gEEC cDNA, and the primers are given in Table 1. The amplified sequences were cloned into pcDNA3.1 (pcDNA3.1-XBP1s and pcDNA3.1-MAP3K2) using the ClonExpress II, one-step cloning kit (Vazyme, Nanjing, China) according to instructions. When gEEC confluence reached 70%, they were transfected individually with pcDNA3.1-XBP1s and pcDNA3.1-MAP3K2 using TurboFect (R0531, Thermo Fisher Science) according to manufacturer's protocol. The empty vector was used as the negative control. Transfectants

Table 1 Primer sequences used in the present study

Target gene	GenBank accession no	Primer sequence 5′-3′	Product size (bp)
Used for qPCR:			
GAPDH	XM_005680968.3	F: GATGGTGAAGGTCGGAGTGAAC R: GTCATTGATGGCGACGATGT	100
GRP78	XM_005687138.3	F: TGAAACTGTGGGAGGTGTCA R: TCGAAAGTTCCCAGAAGGTG	171
ATF6	XM_018046547.1	F: AACCAGTCCTTGCTGTTGCT R: CTTCTTCTTGCGGGACTGAC	224
PERK	XM_018049041.1	F: GGCTAAGAAAGCTGCAAAGCA R: TTTTCACTGAAGCCTCCCAC	171
IRE1α	XM_018065355.1	F: ACTCCCTCAACATCGTTCACAG R: CTCCTTGCAGTCTTCGCTCA	209
XBP1s	XM_018061044.1	F: CCTGCCTGCTGGATGCTTA R: GGGAAAGAGTTCACTGGCAAA	125
E-cadherin	XM_005692180.3	F: GACGTGAACACCCACAATGC R: AAAACTCTCACGGTCCAGCC	141
N-cadherin	XM_018039719.1	F: CAGGGGACATTGGGGACTTC R: GCCCCCAGTCGTTCAGATAG	189
Vimentin	XM_018057155.1	F: TCTGAAGCTGCTAACCGCAA R: CATTTCACGCATCTGGCGTT	147
MAP3K2	XM_018065799.1	GGCCAGTCGACCAGCATTAT TGGTCTGGGGAACTGAAGGA	130
Used for constructing recombinant vector:			
MAP3K2	XM_018065799.1	F: ATGATGGATGATCAGCAAGCTTTGAAC R: CTAGTGGCAGTGCACAAACGTGT	1863
Used for constructing luciferase reporter vector:			
MAP3K2- promoter	XM_018065799.1	F: CCATGGATGGAGGAGCCTGGAGGGC R: CCCGCGCGGCCTGTCACC	2001

were incubated for 12 h then used in the next step of the experiment.

CUT & Tag

CUT & Tag assays were performed using the *CUT & Tag* assay kit (77,552, Cell Signaling Technology, Boston, MA, USA) following the manufacturer's procedure. After XBP1s overexpression, gEECs were harvested by centrifugation and cell suspensions were incubated with concanavalin A beads. XBP1 antibody (diluted 1: 50; ab220783, Abcam, Cambridge, UK) was added and incubated overnight at 4°C. Primary antibody was removed, cells were washed, and goat anti-rabbit IgG (H + L) secondary antibody (1:1000, 35,401, Cell Signaling Technology) was added and incubated for 30 min at RT. The secondary antibody was removed, cells were washed, then the pAG-Tn5 premix was added and incubated for 1 h at RT. The pAG-Tn5 was removed and washed, then the Tagmentation Buffer was added and incubated for 1 h at 37°C. Tagmentation stop solution was added and samples were incubated at 58℃ for 1 h. The tagged chromatin fragments were released into the solution and the samples were centrifuged to obtain the supernatants and the *CUT & Tag* DNAs. The samples were submitted to Novogene Co., Ltd (Beijing, China) for sequencing.

MAP3K2 siRNA transfection

The siRNA targeting goat *MAP3K2* gene (si-MAP3K2) and non-targeting siRNA (si-NC) were synthesized by GenePharma (Shanghai, China), the sequences are presented in Table 2. Cell transfection was performed as described in Sect. " Construction of goat XBP1s knockout (KO) cell lines".

Protein extraction and western blotting

The treated gEECs were collected and whole cell proteins were extracted using the KGP2100 kit (KeyGEN Biotech, China) according to the protocol. Protein concentrations were determined using the bicinchoninic acid assay (KGPBCA; KeyGEN Biotech), followed by SDS-PAGE and immunoblotting to PVDF membranes as described previously [26]. The membranes were blocked, then probed with the following primary antibodies: anti-XBP1 (diluted 1:1000; ab220783, Abcam), anti-E-cadherin (1:1000; 3195, Cell Signaling Technology), anti-N-cadherin (1:1000; 13,116, Cell Signaling Technology), anti-vimentin (1:1000; 5741, Cell Signaling Technology), anti-GRP78 (1:1000; ab21685, Abcam), anti-phospho-IRE1α (1:1000; ab124945, Abcam), and anti-Eif2α (1:1000; ab169528, Abcam),anti- phospho-Eif2α antibody (1:1000; ab32157, Abcam), anti-phospho-p38 (1:1000; CY5262, Abways, Shanghai, China), anti-p38 (1:1000; CY6391, Abways), anti-phospho-ERK1/2 (1:1000; ab169528, Abcam), anti-ERK1/2 (1:1000; ab278538, Abcam), anti-MAP3K2 (1:200; sc1088, Santa Cruz Biotechnology, Dallas TX, USA), anti-β-actin (1:2000; 66,009, Proteintech, Wuhan, China) at 4°C overnight. After removal of primary Ab and washing, the corresponding secondary Abs (1:5000, Zhongshan Golden Bridge Biotechnology) coupled with horseradish peroxidase (HRP) were added and the membranes were incubated at room temperature for 1 h. Afterwards, the protein bands were visualized using a gel imaging system (Tanon Biotech, Shanghai, China) and quantified by Quantity One software (Bio-Rad Laboratory, Hercules, CA, USA).

RNA extraction and real-time quantitative PCR (RT-qPCR)

Following treatment, the gEECs were collected and total RNA was extracted using TRIzol (TaKaRa Bio, Inc., Dalian, China). The RNA was converted to cDNA by reverse transcription using a PrimeScript™ RT reagent kit with gDNA Eraser (TaKaRa Bio, Inc.). The qPCR was conducted using ChamQ SYBR qPCR master mix (Vazyme Biotech Co., Ltd., Nanjing, China) on a Bio-Rad CFX96 system (Bio-Rad Laboratories, Inc., CA, USA), and the primers are presented in Table 1. GAPDH was utilized as invariant control, and the relative expression of each gene was determined by the $2^{-\Delta\Delta Ct}$ method.

Dual-luciferase reporter assay system

Previously described protocols were followed [27]. Briefly, the promoter sequence of *MAP3K2* (-2001 to -1) was amplified from the genomic DNA of gEECs with the primers shown in Table 1. The 2001 bp fragment of the *MAP3K2* promoter was cloned into the PGL4.10 vector (*MAP3K2*-Luc) via seamless cloning (ClonExpress II, one-step cloning kit). The *MAP3K2*-Luc and PRL-CMV plasmids were co-transfected with pcDNA3.1 or pcDNA3.1-XBP1s using TurboFect, respectively. The cells were harvested 36 h post-transfection and analyzed using the Dual-Luciferase reporter assay system (Promega, Madison, WI, USA) and SPARK multimode

Table 2 siRNA sequence

siRNA Name	Sequences(5′-3′)
siMAP3K2-1	GUCUAUGGAUCUGCAUUAUTT
	AUAAUGCAGAUCCAUAGACTT
siMAP3K2-2	CCCACUAGUAGAGAUAGAATT
	UUCUAUCUCUACUAGUGGGTT
siMAP3K2-3	GGCUCCAUUAAGGACCAAUTT
	AUUGGUCCUUAAUGGAGCCTT
siNC	UUCUCCGAACGUGUCACGUTT
	ACGUGACACGUUCGGAGAATT

microplate reader (Tecan, Mannedorf, Switzerland) to determine luciferase activity. Renilla luciferase was used as the control for normalization.

Molecular docking

We commissioned Phadcalc (Chengdu, China) to conduct molecular docking assays of the transcription factor XBP1s protein with the *MAP3K2* promoter sequence. The proteins and DNA sequences were modeled separately using the AlphaFold3 program, followed by docking using the HDCOK program. The molecular docking scoring was calculated based on the ITScorePP or ITScorePR iterative scoring function. The more negative the docking score, the greater the binding possibility and stronger the interaction for that binding model. A confidence score was defined to indicate the binding possibility of the two molecules as follows:

$$\text{Confidence score} = 1.0/[1.0 + e0.02^{*}(\text{Docking\_Score} + 150)]$$

When the confidence score is higher than 0.7, the two molecules are very likely to bind to each other; when the confidence score is between 0.5 and 0.7, the two molecules are likely to bind; when the confidence score is lower than 0.5, the two molecules are unlikely to bind. The results of this molecule docking are shown in Table 3. As evidenced by the docking score and confidence score in the table, the complex model obtained by docking exhibited a high degree of confidence.

Immunohistochemistry

The prepared uterine sections were heated at 65°C for 45 min, deparaffinized in xylene, rehydrated in descending ethanol, antigenically repaired in sodium citrate buffer and incubated with 3% hydrogen peroxide solution to inactivate endogenous peroxidase activity. Non-specific reactions were blocked with bovine serum albumin (BSA) for 1 h at RT, then sections were incubated with primary antibodies against XBP1, E-cad, N-cad, and MAP3K2, overnight at 4°C, followed by incubation with the corresponding HRP-conjugated secondary antibody for 30 min at RT. Lastly, the sections were incubated with 3, 3′-diaminobenzidine (DAB) as HRP substrate for 1 min and then stained with hematoxylin. The sections were observed and digitally photographed with a visual-light microscope (Nikon, Tokyo, Japan).

Table 3 Docking results

Receptors	Ligands	Docking Score	Confidence Score
DNA	Protein	-204.30	0.7476

Data statistics and analysis

Unless otherwise stated, all data are expressed as the mean ± SEM, and statistical significance was determined using Student's *t*-test when comparing two groups of data. Analysis of variance (ANOVA) was performed using GraphPad Prism version 8.0.1 (GraphPad Software Inc., San Diego, CA). Differences were considered statistically significant for $p < 0.05$. At least three independent replications were performed for each experiment.

Results

Chronic endometritis induces the EMT

Uterine tissues were obtained from healthy dairy goats and compared with similar tissues from endometritic dairy goats. Their respective inflammation levels were characterized and divided into healthy and endometritic groups (unpublished data). Analysis of the immunohistochemical results showed that E-cad expression in EECs was significantly decreased in endometritic tissues, whereas N-cad exhibited the opposite trend (Fig. 1A). The expression of E-cad protein was significantly lower in endometritic tissues compared to healthy tissues, while N-cad and VIM proteins were significantly higher ($P < 0.01$; Fig. 1B-C). These findings demonstrate that EMT occurs in endometritis.

LPS induces the EMT in a time-dependent manner

Previous research in our laboratory showed that treatment of gEECs with LPS (5 μg/mL) for 24 h did not affect cell viability [24]. Therefore, gEECs were treated with LPS for different lengths of time up to 24 h. Compared with the control group, LPS treatment for 12 h significantly suppressed mRNA expression of the epithelial marker, E-cad, and with prolonged LPS treatment it reached its lowest level at 24 h ($P < 0.01$; Fig. 1H). Concurrently, the mRNA expression of the mesenchymal markers, N-cad and VIM, was significantly increased by LPS treatment in a time-dependent manner and reached its highest point at 24 h ($P < 0.01$; Fig. 1I-J). The protein expression showed similar results: LPS treatment suppressed the protein expression of

(See figure on next page.)

Fig. 1 Endometritis induces the epithelial-mesenchymal transition (EMT). **A** Immunohistochemical analysis of the expression of the epithelial polarity marker E-cadherin and the mesenchymal marker N-cadherin. **B**-**C** Western blotting analysis for E-cadherin, N-cadherin, and vimentin proteins; β-actin levels are shown as the loading control. **D**-**G** E-cad, N-cad, and Vim expression in gEECs was analyzed using western blotting and quantitated by densitometry. **H**-**J** The mRNA levels of *E-cad, N-cad,* and *VIM* in gEECs, normalized to the levels of *GAPDH*, were quantified using RT-qPCR. Scale bar = 200 μm. Data values are means ± SEM of three independent experiments. *$P < 0.05$; **$P < 0.01$; ***$P < 0.001$

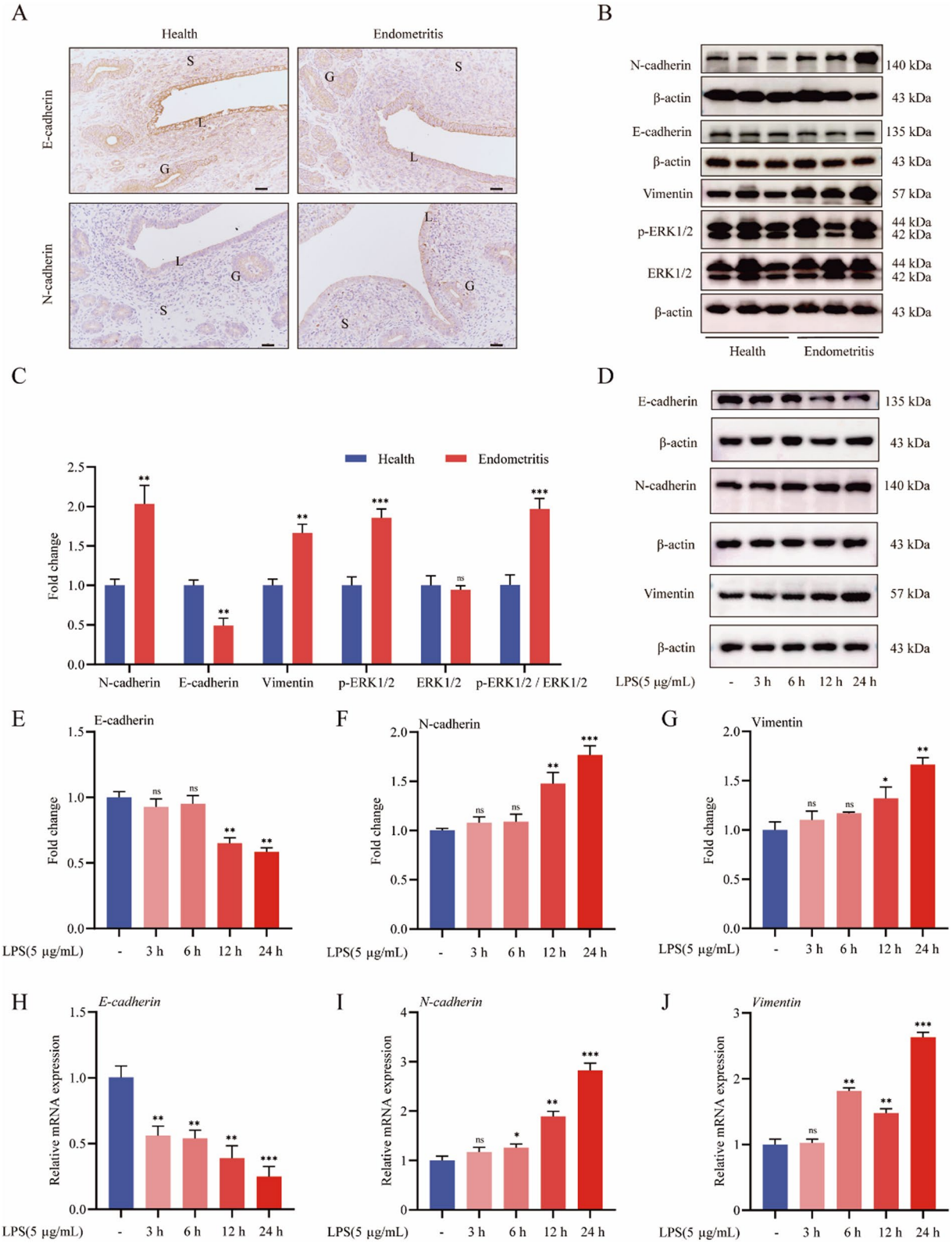

Fig. 1 (See legend on previous page.)

E-cad and promoted the protein expression of N-cad and VIM in a time-dependent manner ($P<0.01$; Fig. 1D-G). These results suggest that sustained LPS treatment induces the EMT in gEECs.

Elevated XBP1s expression in chronic endometritis-induced EMT

Our immunohistochemical results showed that the expression of *XBP1s* was significantly increased in endometritic tissues, compared with healthy tissues ($P<0.001$; Fig. 2A-C). Interestingly, we found that not only XBP1s protein but also unspliced XBP1 protein was significantly increased in endometritis tissues (Fig. 2B-C). In addition, our previous study reported that ERS could be activated by LPS treatment of gEECs for 6 h [28]. However, whether ERS is involved in the EMT under chronic inflammation has not been determined; therefore, we measured the changes in ERS-related genes after inducing the EMT in gEECs by LPS treatment. As shown in Fig. 2D-F, LPS treatment significantly increased the protein expression of the ERS marker GRP78 ($P<0.001$), as well as phosphorylation of the ERS-related proteins, IRE1α ($P<0.01$) and Eif2α ($P<0.01$) and the splicing of XBP1s protein ($P<0.01$). Consistent with the protein expression levels, LPS treatment also significantly increased the mRNA expression of *GRP78*, *IRE1α*, *ATF6*, *PERK*, *XBP1s* ($P<0.001$; Fig. 2G).

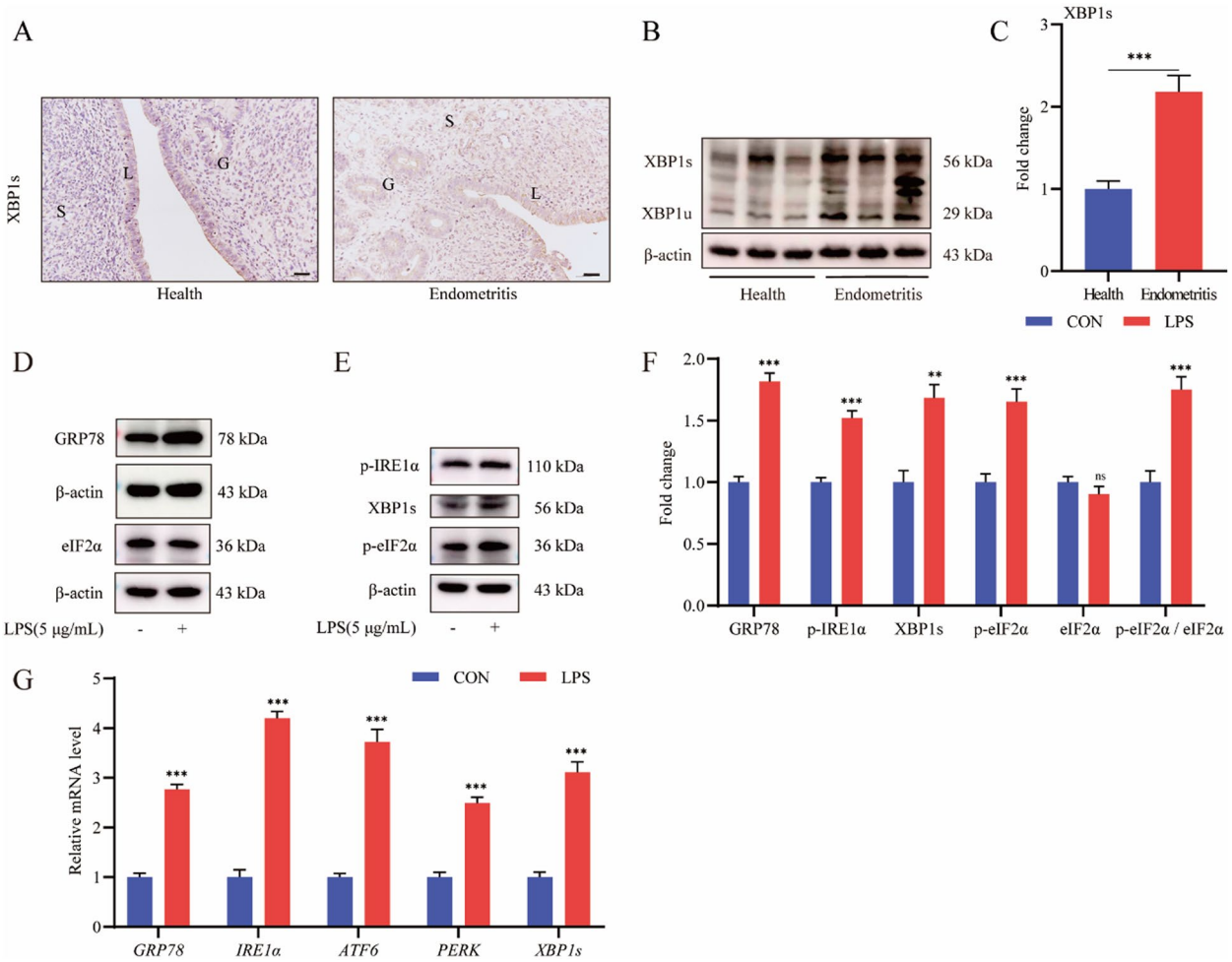

Fig. 2 Endoplasmic reticulum stress (ERS) is activated in both endometritis tissue and LPS-treated gEECs. **A**-**C** The expression levels of XBP1s protein were analyzed by immunohistochemistry and western blotting. **D**-**F** The relative protein expression of GRP78, XBP1s, phospho-IRE1α, and phospho-eIF2α were determined by western blotting and quantified by densitometry. **G** Relative mRNA expression of *GRP78*, *IRE1α*, *ATF6*, *PERK*, and *XBP1s* was normalized to the level of *GAPDH* as quantified by RT-qPCR. Scale bar = 200 μm. Data values are means ± SEM of three independent experiments. *$P<0.05$; **$P<0.01$; ***$P<0.001$

Effects of XBP1s on the LPS-induced EMT

XBP1s promotes the LPS-induced EMT

The accumulated evidence supports the hypothesis that *XBP1s* is a key downstream component of ERS and plays an important role in various physiological and pathological processes [29, 30]. The present study found that the expression of *XBP1s* was significantly increased in both endometritic tissues and LPS treatment-induced EMT in gEECs. Therefore, we hypothesized that *XBP1s* might play a key role in gEECs EMT, so we knocked out *XBP1s* (XBP1s KO) in gEECs (Fig. S1A-B). Compared with WT, XBP1s KO significantly inhibited the expression of N-cad and VIM, and the decrease in E-cad ($P < 0.001$; Fig. 3A-F and H). In addition, XBP1s KO also significantly inhibited the migration of gEECs ($P < 0.05$; Fig. 3G and I).

We further explored the effect of XBP1s on the EMT in gEECs by overexpressing *XBP1s*, which resulted in a significant decrease in the expression of E-cad, while the expression of N-cad and VIM increased significantly ($P < 0.01$; Fig. 4A-F and H). Overexpression of *XBP1s* also significantly promoted the migration of gEECs ($P < 0.01$; Fig. 4G and I).

The MAPK/ERK pathway is a downstream target of XBP1s

Because XBP1s exerts its function as a transcription factor, we performed a *CUT & Tag* assay of XBP1s to screen its downstream target genes. The *CUT & Tag* analysis identified 4723 peaks that significantly bound XBP1s. Functional annotation analysis showed that nearly 70% of the XBP1s binding peaks were located in the promoter region, and 66.48% of the binding peaks were within 1 kb of the promoter region (Fig. 5A-C). Next, KEGG enrichment analysis was performed on the target genes corresponding to the binding peaks, and it was found that the target genes of XBP1s were mainly enriched in endoplasmic reticulum protein expression, protein and RNA transport, fatty acid metabolism, autophagy, the MAPK/ERK and other pathways (Fig. 5D-E).

We hypothesized that XBP1s might function through the MAPK/ERK pathway in LPS-induced EMT and measured the activation of the MAPK/ERK pathway in goat endometritic tissues and after the LPS-induced EMT. Phosphorylation of p38 and ERK were significantly increased in endometritic tissues compared with healthy tissues ($P < 0.01$; Fig. 1B-C; Fig. 6A-B). Similar results were found in gEECs, where the phosphorylation of p38 was significantly increased by LPS treatment compared with control ($P < 0.01$; Fig. 6C-D). In addition, ERK phosphorylation was also significantly increased ($P < 0.01$; Fig. 6C-D). Pretreatment with DHC activated the MAPK/ERK pathway while PD98056 inhibited it. PD98056 pretreatment was also found to significantly inhibit N-cad and VIM expression and significantly inhibit the decrease in E-cad; while DHC pretreatment had the opposite effect ($P < 0.05$; Fig. 6E-K).

XBP1s promotes LPS-induced EMT through the MAPK/ERK pathway

We next determined if XBP1s functioned through the MAPK/ERK pathway. Overexpression of XBP1s significantly increased the phosphorylation of p38 and ERK1/2 ($P < 0.001$; Fig. S2A-B), while XBP1s KO significantly decreased the phosphorylation of these proteins ($P < 0.01$; Fig. S2C-D).

To further test our hypothesis, PD98059-mediated inhibition of the MAPK/ERK pathway was found to significantly reverse the effects of XBP1s and to significantly suppress the decrease of *E-cad* and the increase of *N-cad* and *VIM* caused by overexpression of XBP1s ($P < 0.01$; Fig. 4 A-F and H). Coincidentally, activation of the MAPK/ERK pathway using DHC significantly promoted the increase of *E-cad* and the decrease of *N-cad* and *VIM* caused by XBP1s KO ($P < 0.01$; Fig. 3A-F and H). These results suggest that XBP1s facilitates the LPS-induced EMT by promoting the MAPK/ERK pathway.

MAP3K2 mediates the XBP1s promotion of MAPK/ERK pathway activation to facilitate LPS-induced EMT

XBP1s directly regulate MAP3K2 expression

In the *CUT & Tag* assay of XBP1s, we found that *MAP3K2*, a key gene of the MAPK/ERK pathway, functioned as a target gene of XBP1s (Table S1). Then we verified that the mRNA and protein expression of MAP3K2 was significantly increased after overexpression of XBP1s; and XBP1s KO significantly inhibited the expression of *MAP3K2* ($P < 0.001$; Fig. 7A-E). To further confirm that XBP1s functioned by directly binding to the *MAP3K2* promoter, we co-transfected HEK 293T cells with dual-luciferase reporter vectors containing *MAP3K2*-promoter (2001 bp) and either pcDNA3.1-XBP1s or pcDNA3.1. The transcriptional activity of *MAP3K2* was significantly increased following transfection with pcDNA3.1-XBP1s compared with that in the pcDNA3.1 group ($P < 0.001$; Fig. 7F). To determine whether *XBP1s* promoted *MAP3K2* transcription by binding to specific sites within its promoter, we performed molecular docking assays. Molecular docking of the XBP1s protein model (Fig. 7G) with the *MAP3K2* promoter sequence model (Fig. 7H) revealed the existence of multiple modes of interaction between *XBP1s* and *MAP3K2* sequences including electrostatic, hydrogen-bonded, carbon-hydrogen-bonded and hydrophobic interactions (Fig. 7I).

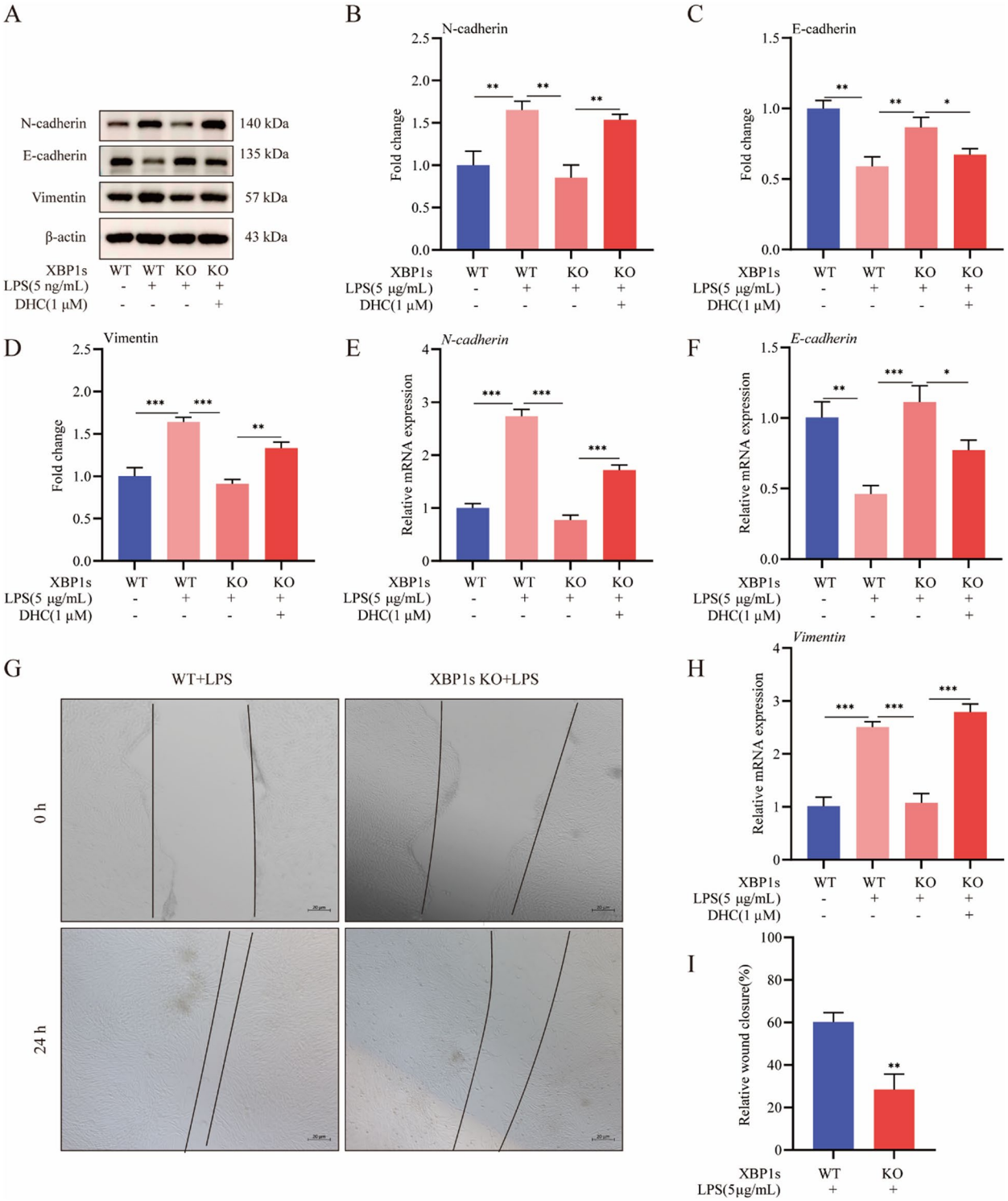

Fig. 3 XBP1s KO regulates the LPS-induced EMT through inhibition of the MAPK/ERK pathway. Goat endometrial epithelial cells (gEECs) were treated with LPS for 24 h after 1 μM DHC treatment for 2 h. **A**-**D** Western blotting results and densitometric analysis of E-cad, N-cad, and VIM with XBP1s KO. **E**–**F** and **H** The mRNA levels of *E-cad, N-cad and VIM* were normalized to the level of *GAPDH* after knockout of *XBP1s*. **G** and **I** LPS-induced changes in migration of gEECs following knockout of *XBP1s*. Scale bar = 20 μm. Data values are means ± SEM of three independent experiments. **P* < 0.05; ***P* < 0.01; ****P* < 0.001

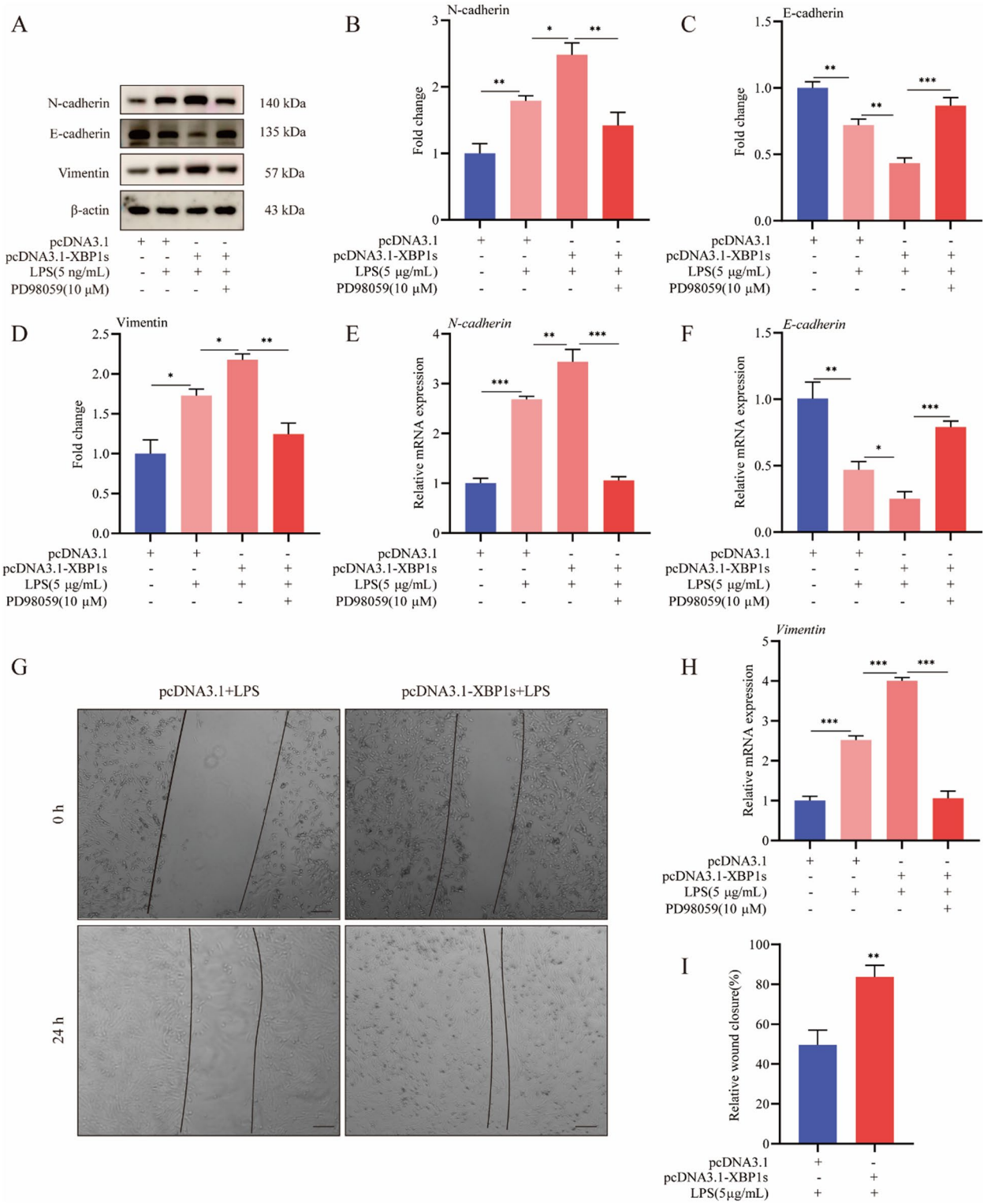

Fig. 4 XBP1s overexpression regulates the LPS-induced EMT through activation of the MAPK/ERK pathway. Goat endometrial epithelial cells (gEECs) were treated with LPS for 24 h after 10 μM PD98059 treatment for 2 h. **A**-**D** Western blotting results of E-cad, N-cad, and VIM after overexpression of XBP1s. **E**–**F** and **H** The mRNA levels of *E-cad, N-cad and VIM* were normalized to the levels of *GAPDH* after overexpression of *XBP1s*. **G** and **I** LPS-induced changes in migration of gEECs following overexpression of *XBP1s*. Scale bar = 20 μm. Data values are means ± SEM of three independent experiments. **P* < 0.05; ***P* < 0.01; ****P* < 0.001

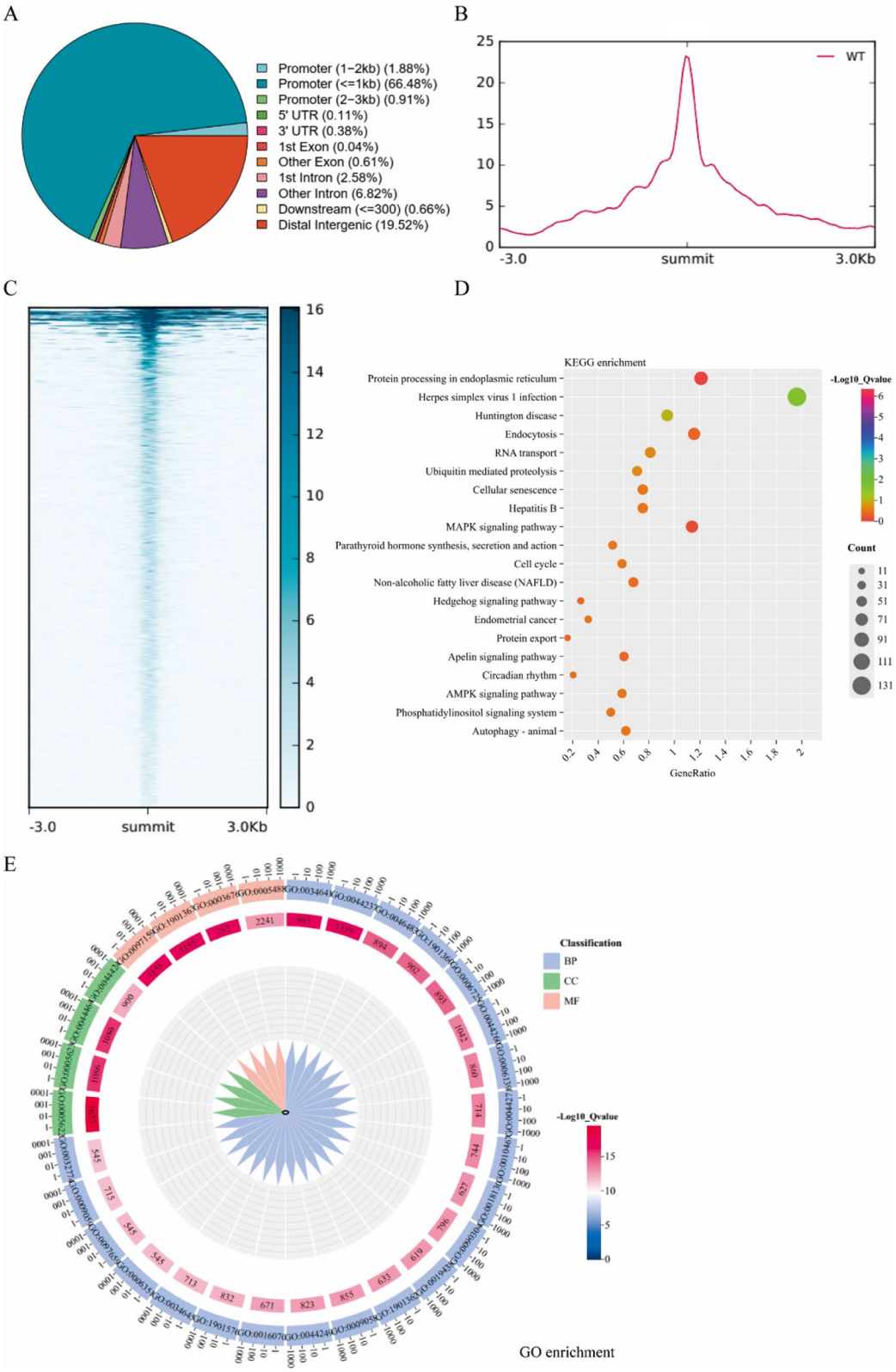

Fig. 5 *CUT & Tag* assay reveals downstream gene targets of XBP1s. **A** Genome-wide distribution of XBP1s binding peaks. **B** Metagene analyses of XBP1s coverage at transcription start sites (TSS). Regions selected from TSS (±3 kb). **C** The binding density of XBP1s was visualized using deepTools. The heatmap shows the *CUT & Tag* counts on different peaks, ordered by signal strength. **D**-**E** KEGG and GO enrichment analysis of target genes downstream of XBP1s

MAP3K2 facilitates the LPS-induced EMT by promoting the MAPK/ERK pathway

Next, we explored the expression of MAP3K2 in endometritic tissues and found that it was significantly upregulated, consistent with activation of the MAPK/ERK pathway ($P < 0.001$; Fig. 6A-B). Next, we found that MAP3K2 overexpression significantly increased LPS-induced phosphorylation of p38 and ERK proteins ($P < 0.01$; Fig. S3); significantly promoted the migration of gEECs, significantly increased the expression of *N-cad* and *VIM* and significantly suppressed the expression of *E-cad*, whereas the use of PD98059 significantly inhibited this effect ($P < 0.01$; Fig. 8; Fig. S1B-D). MAP3K2 knockdown significantly inhibited LPS-induced activation of the MAPK/ERK pathway and the EMT, which was reversed by DHC ($P < 0.01$; Fig. 9; Fig. S1E-G). In summary, our current results suggest that XBP1s promotes the MAPK/ERK pathway by targeting *MAP3K2*, which in turn promotes the LPS-induced EMT.

Discussion

The animal uterus is an organ with complex immune functions that are required to maintain an immune-tolerant environment during development of the semi-homozygous fetus, as well as to maintain its ability to monitor and respond to infectious agents [31]. However, after delivery, the uterus is exposed to bacterial contamination, tissue damage and other adverse factors that predispose it to endometritis, which can cause significant economic losses to the livestock industry [32]. Previous studies have reported that endometritis in ruminants mainly results from chronic inflammation or chronic inflammation that developed from acute inflammation [33, 34]; therefore, it is crucial to focus on chronic persistent inflammation of the uterus in animals. In addition, the EMT can be induced under chronic persistent inflammation, leading to loss of epithelial cell polarity [35]. In the present study, we found a significant decrease in the expression of the polarity marker, E-cadherin in endometrial epithelial cells (EECs) and a significant increase in the expression of the mesenchymal markers, N-cadherin and vimentin in tissues of dairy goats with persistent endometritis. This suggests that EMT occurs in EECs during endometritis. Treatment of goat EECs with LPS revealed that persistent LPS exposure (> 12 h) induced EMT, significantly inhibited the expression of *E-cad*, significantly increased the expression of *N-cad* and *VIM*, and disrupted the epithelial polarity of gEECs. This is similar to previous studies in which LPS treatment induced an inflammatory response in mammary epithelial cells of dairy cows accompanied by the development of the EMT [36]. It was also reported that SARA-induced translocation of LPS into the bloodstream induced mastitis, leading to disruption of mammary epithelial cell polarity [37]. However, the mechanism of endometritis-induced EMT remains unclear.

Many studies have reported that XBP1s is involved in various pathophysiological processes as an effector of ERS, making it a potential therapeutic target for disease treatment [38, 39]; therefore, we hypothesized that the transcription factor, XBP1s, may mediate the endometritis-induced EMT process. We found that *XBP1s* expression was significantly increased in endometritis tissues, and persistent LPS treatment significantly increased *XBP1s* expression in gEECs. Interestingly, we also detected the expression of ERS-related genes, with a significant increase in the expression of the ERS marker, GRP78. In addition, phosphorylation of IRE1α and EIF2α proteins was also significantly increased. Our previous study also indicated that splicing of XBP1u and expression of XBP1s were increased through the TLR4-ERS-IRE1a pathway in the early stage (6 h) of LPS treatment of gEECs [28]. In this study, we showed that XBP1s was similarly involved in persistent LPS-induced EMT. Overexpression of *XBP1s* in gEECs significantly facilitated LPS-induced EMT, with a significant decrease in E-cad and a significant increase in N-cad and VIM, along with a significantly enhanced migration rate of gEECs. Conversely, XBP1s KO inhibited EMT. Therefore, we determined that the transcription factor, XBP1s, plays an important role in endometritis-induced EMT. This is similar to previous studies in which ERS mediated cellular damage through activation of *XBP1s* [40].

XBP1s contains basic leucine zip structures and is the critical transcription factor of the ERS pathway. Therefore, we performed a *CUT & Tag* assay on *XBP1s* to explore its role in persistent LPS-induced EMT. KEGG enrichment analysis revealed that the target genes of XBP1s were enriched in the MAPK/ERK pathway. We measured significant activation of the MAPK/ERK pathway in both endometritic tissues and persistent LPS-treated gEECs, with significantly increased

(See figure on next page.)

Fig. 6 LPS treatment activates the MAPK/ERK pathway. **A**-**B** The expression of phosphorylated p38 protein in endometritic tissues was analyzed and determined by western blotting. **C**-**D** Activation of the MAPK/ERK pathway in LPS-treated gEECs. **E**–**H** Relative protein expression of E-cad, N-cad, and VIM after activation or inhibition of the MAPK/ERK pathway. **I**-**K** The mRNA levels of *E-cad, N-cad* and *VIM* were normalized to the level of *GAPDH*. Data values are means ± SEM of three independent experiments. *$P < 0.05$; **$P < 0.01$; ***$P < 0.001$ vs. control group. $^{\#}P < 0.05$; $^{\#\#}P < 0.01$; $^{\#\#\#}P < 0.001$ vs. other group

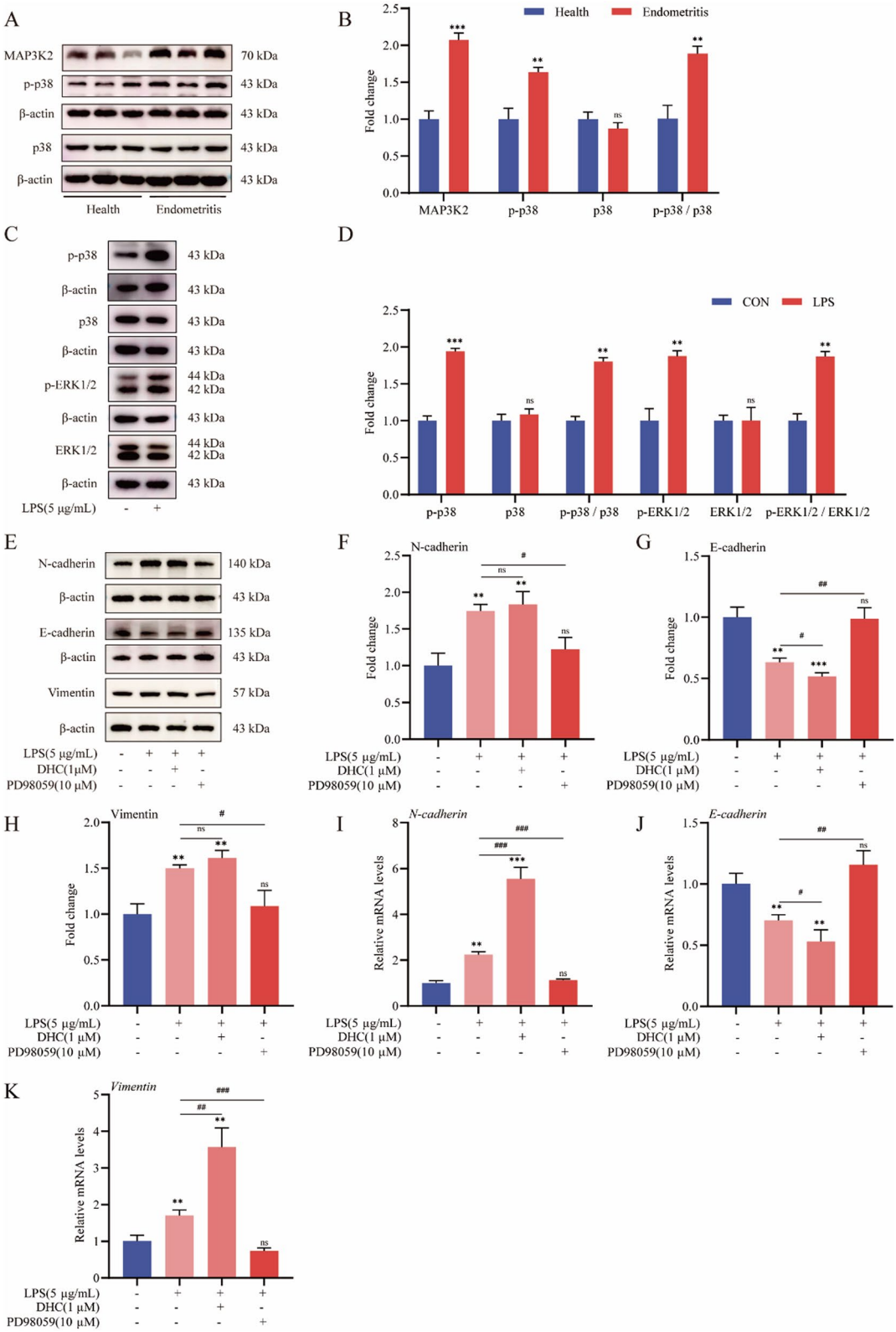

Fig. 6 (See legend on previous page.)

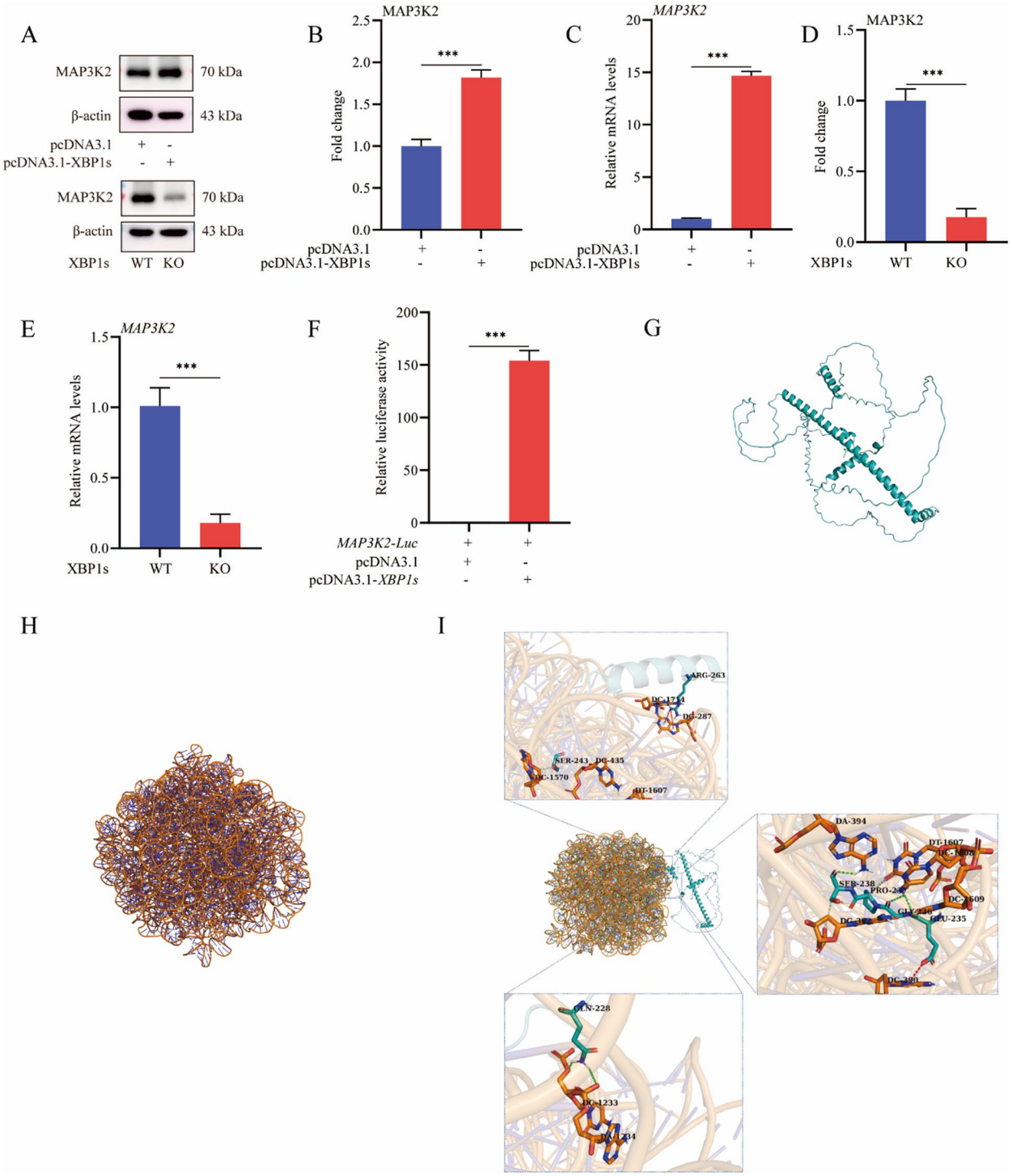

Fig. 7 XBP1s regulates *MAP3K2* transcription. **A**-**E** The influence of overexpression or knockout of XBP1s on MAP3K2. **F** The relative luciferase activity of MAP3K2-Luc was measured. **G**-**I** Molecular docking and molecular dynamics of the conjugation between XBP1s and *MAP3K2*: **(G)** *MAP3K2* promoter structure, (**H)** XBP1s protein structure, and (**I)** *MAP3K2* promoter interaction with XBP1s protein. Orange represents DNA bases, and blue represents amino acids. Green dashed lines indicate hydrogen bonding interactions, cyan dashed lines indicate hydrocarbon bonding interactions, and red dashed lines indicate electrostatic interactions. Data values are means ± SEM of three independent experiments. *$P < 0.05$; **$P < 0.01$; ***$P < 0.001$

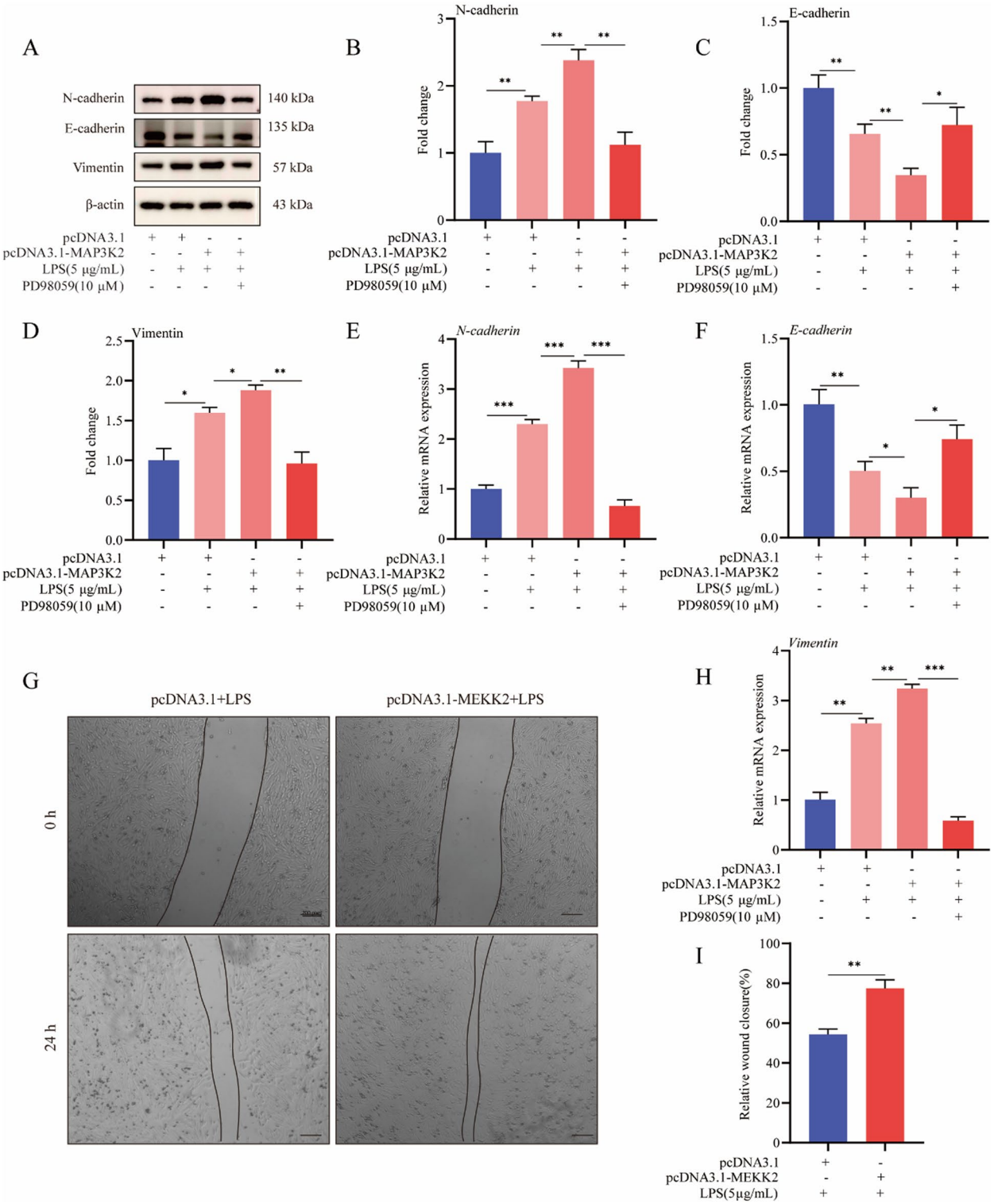

Fig. 8 *MAP3K2* overexpression regulates the LPS-induced EMT through activation of the MAPK/ERK pathway. **A**-**D** Western blotting results and densitometric analysis of E-cad, N-cad, and VIM after overexpression of MAP3K2. **E–F** and **H** The mRNA levels of *E-cad, N-cad and VIM*, normalized to the level of *GAPDH*, were determined using RT-qPCR after overexpression or knockdown of *MAP3K2* in gEECs. **G** and **I)** Changes in LPS-induced migration of gEECs after overexpression of *MAP3K2*. Scale bar = 20 μm. Data values are means ± SEM of three independent experiments. **P* < 0.05; ***P* < 0.01; ****P* < 0.001

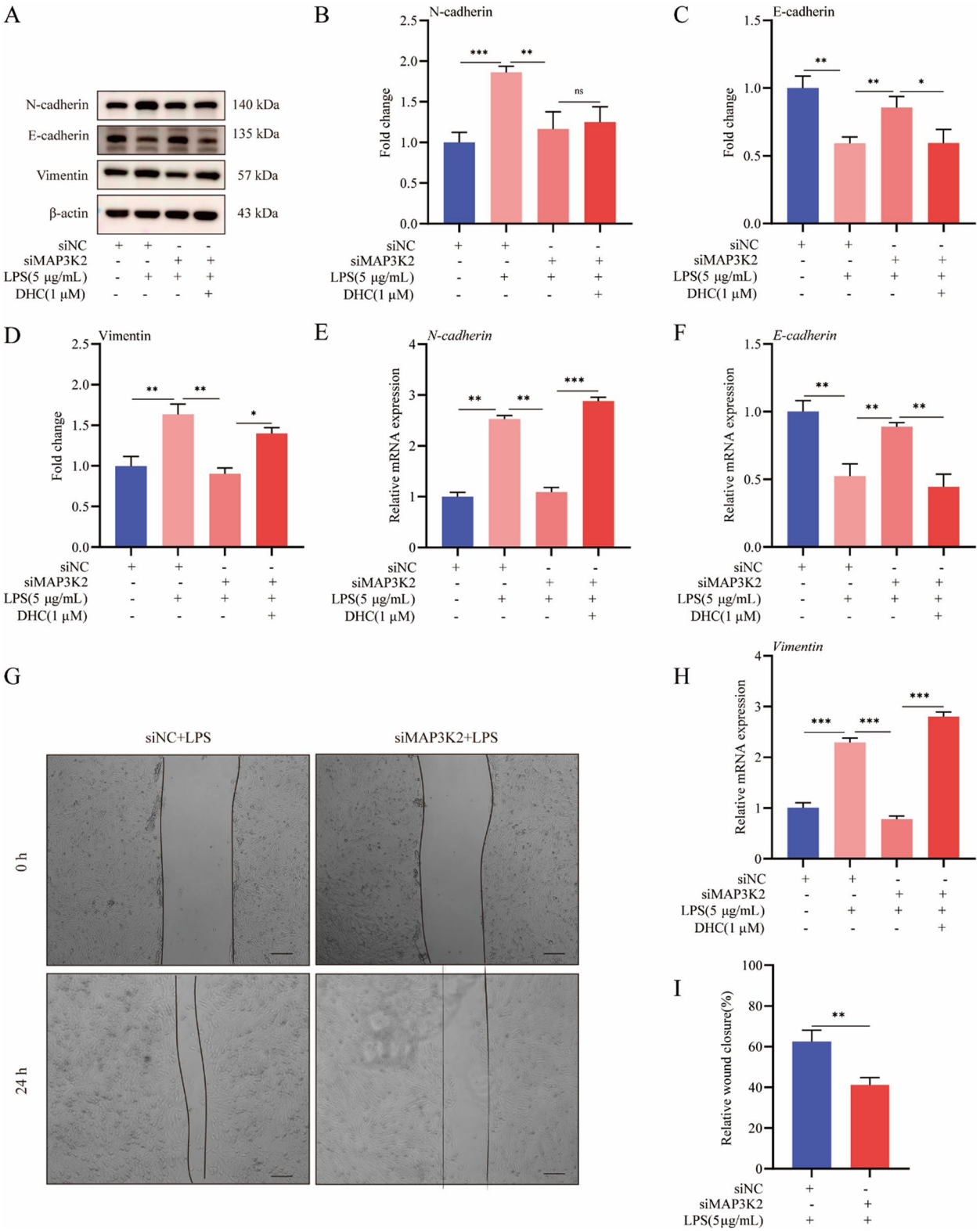

Fig. 9 *MAP3K2* knockdown regulates the LPS-induced EMT through inhibition of the MAPK/ERK pathway. **A**-**D** Western blotting results and densitometry of E-cad, N-cad, and VIM, with MAP3K2 knockdown. **E**–**F** and **H** The mRNA levels of *E-cad, N-cad and VIM* were determined using RT-qPCR after knockdown of *MAP3K2* in gEECs. **(G** and **I)** Changes in LPS-induced migration of gEECs after knockdown of *MAP3K2*. Scale bar = 20 μm. Data values are means ± SEM of three independent experiments. **P* < 0.05; ***P* < 0.01; ****P* < 0.001

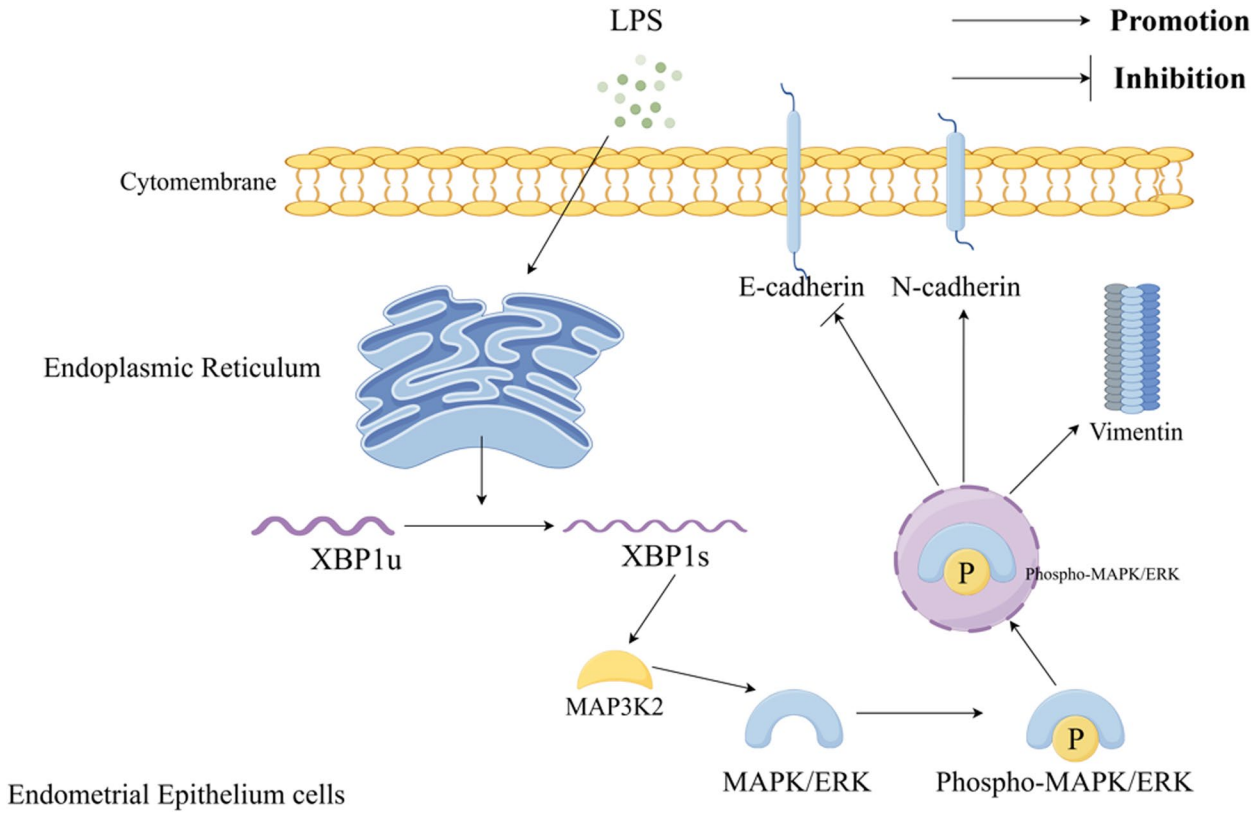

Fig. 10 XBP1s promotes endometritis-induced EMT

phosphorylation of p38 and ERK1/2 proteins. Activation of the MAPK/ERK pathway with DHC or inhibition with PD98059 significantly increased or inhibited the LPS-induced EMT, respectively, suggesting that LPS induced EMT through the MAPK/ERK pathway. Inhibition of the MAPK/ERK pathway has been demonstrated to prevent LPS-induced cellular damage.

This supported our study results, and we hypothesized that the action of XBP1s is mediated through the MAPK/ERK pathway. Overexpression of XBP1s significantly increased the LPS-induced phosphorylation of p38 and ERK1/2 proteins and activated the MAPK/ERK pathway, while XBP1s KO showed the opposite result. We also pretreated gEECs with PD98059 or DHC and found that PD98059 significantly inhibited the LPS-induced EMT after overexpression of XBP1s, significantly suppressed the decrease of E-cad, the expression of *N-cad* and *VIM*, and reversed the effects of XBP1s; DHC pretreatment showed the opposite results, supporting our hypothesis, that XBP1s acts through the MAPK/ERK pathway in LPS-induced EMT. In line with the present study. Inhibition of ERS-induced XBP1s reduced activation of the MAPK/ERK pathway, which reduced apoptosis and protected cells [41]. Thus, these results suggest that XBP1s promoted the EMT through the MAPK/ERK pathway in gEECs continuously exposed to LPS.

To further explore the mechanism of XBP1s action, we analyzed the *CUT & Tag* assay data and found that *MAP3K2*, an important component of the MAPK/ERK pathway, may be a target gene of XBP1s. We found that the expression pattern of MAP3K2 in both endometritic tissues and gEECs showed a positive correlation with the expression of XBP1s. Therefore, we hypothesized that XBP1s activated the MAPK/ERK pathway through MAP3K2. We used a dual-luciferase reporter assay to confirm that XBP1s significantly increased the promoter activity of *MAP3K2*. We also performed molecular docking assays and found multiple modes of interaction between XBP1s protein and the *MAP3K2* promoter sequences such as electrostatic, hydrogen-bonding, carbon-hydrogen-bonding and hydrophobic interactions. However, the binding site we validated was not the classical recognition sequence of basic leucine zip proteins (ACGT), which is inconsistent with a previous study [42]. We speculate that the promoter sequences of the XBP1s-bound target genes may be species-conserved and may be dissimilar between species. Taken together, these data provide evidence that the MAPK/ERK pathway component, *MAP3K2*, is a target gene of *XBP1s*.

It was previously suggested that MAP3K2 was essential for the activation of the MAPK/ERK pathway [43].

In addition, it has also been found that MAP3K2 and MAPK/ERK pathway activation showed a positive correlation in transcriptome sequencing analysis of LPS-induced cellular inflammation models [44]. Based on these findings, we further explored the mechanism of MAP3K2 action in the LPS-induced EMT. It was found that overexpression of MAP3K2 in gEECs significantly inhibited the expression of *E-cad*, increased the expression of *N-cad* and *VIM*, increased the phosphorylation of p38 and ERK1/2 proteins, and facilitated LPS-induced migration, whereas inhibition of the MAPK/ERK pathway with PD98059 significantly reversed the effects of MAP3K2. The knockdown of MAP3K2 significantly inhibited LPS-induced EMT, and DHC pretreatment reversed the effects of the MAP3K2 knockdown. Thus, we conclude that MAP3K2 facilitates the LPS-induced EMT by activating the MAPK/ERK pathway. This is similar to a previous study in which targeted disruption of *MAP3K2* expression inhibited activation of the MAPK/ERK pathway [45].

Conclusions

Our results elucidated the mechanism of XBP1s involvement in the LPS-induced EMT. LPS treatment induced ERS and activated *XBP1s*, which promoted *MAP3K2* transcription through direct binding of XBP1s protein to the promoter. This activated the MAPK/ERK pathway and facilitated the EMT, whereas XBP1s KO inhibited LPS-induced EMT (Fig. 10). We provide evidence that MAP3K2 mediates the involvement of the ERS pathway key transcription factor, XBP1s, in the LPS-induced EMT. These results broaden our understanding of the role of XBP1s in the regulation of uterine biological functions.

Abbreviations

XBP1s	X-box binding protein 1 splicing variant
EMT	Epithelial-mesenchymal transition
ERS	Endoplasmic reticulum stress
E-cad	E-cadherin
N-cad	N-cadherin
VIM	Vimentin
LPS	Lipopolysaccharide
gEECs	Goat endometrial epithelial cells
UPR	Unfolded protein response
IRE1α	Inositol-requiring enzyme 1α
ATF6	Activating transcription factor 6
PERK	Protein kinase R (PKR)-like ER kinase
GRP78	Glucose regulated protein 78
PBS	Phosphate-buffered saline
hTERT	Human telomerase reverse transcriptase
DHC	Dehydrocorydaline chloride
DF12	Dulbecco's modified Eagle's medium (DMEM)/F-12
DMEM	Dulbecco's modified Eagle's medium
FBS	Fetal bovine serum
SDS-PAGE	Sodium dodecyl sulfate polyacrylamide gel electrophoresis
GAPDH	Glyceraldehyde-3-phosphate dehydrogenase

Supplementary Information

The online version contains supplementary material available at https://doi.org/10.1186/s12964-025-02050-0.

Supplementary Material 1: Figure S1. Validation of vector expression efficiency in gEECs. (A) Genome sequencing of *XBP1s* knockout cells. (B-D) The knockout efficiency of *XBP1s* in gEECs and the overexpression efficiency of *MAP3K2* were verified. (E-G) Validation of knockdown efficiency of MAP3K2 in gEECs. Data values are means ± SEM of three independent experiments. **P* < 0.05;***P* < 0.01; ****P* < 0.0. Figure S2. Effect of XBP1s on the MAPK/ERK pathway in gEECs. (A-B) Western blotting results of p38 and ERK1/2 phosphorylation levels in control and overexpression of XBP1s gEECs. (C-D) Western blotting results of p38 and ERK1/2 phosphorylation levels in *XBP1s* KO gEECs. Data values are means ± SEM of three independent experiments. **P* < 0.05; ***P* < 0.01; ****P*< 0.001. Figure S3. Effect of MAP3K2 on the MAPK/ERK pathway in gEECs. (A-D) Western blotting results of p38 and ERK1/2 phosphorylation levels in control and overexpression of MAP3K2 gEECs or in MAP3K2 knockdown gEECs. Data values are means ± SEM of three independent experiments. **P* < 0.05; ***P* < 0.01; ****P*< 0.001

Authors' contributions

Kangkang Gao: designed the experiments, performed experiments, analyzed the data, interpreted the experimental results, prepared figures, drafted the manuscript. Mengqi Si: performed experiments. Xinxi Qin: performed experiments. Beibei Zhang: analyzed the data. Zongjie Wang: analyzed the data. Pengfei Lin: analyzed the data, interpreted the experimental results. Huatao Chen: analyzed the data, interpreted the experimental results. Aihua Wang: interpreted the experimental results. Yaping Jin: designed the experiments, analyzed the data, interpreted the experimental results, prepared figures, drafted the manuscript, supervised the project and edited the manuscript. All authors approved the final version of this manuscript.

Funding

This study was supported by The National Key R&D Program of China (Grant No. 2023YFD1801100); Shaanxi Livestock and Poultry Breeding Double-chain Fusion Key Project (Grant No. 2022GD-TSLD-46); The Key R&D Program of Ningxia Hui Autonomous Region (Grant No. 2018BBF33001).

Data availability

Data is provided within the manuscript or supplementary information files.

Declarations

Ethics approval and consent to participate

Experiments and surgical procedures were performed according to protocols approved by the Northwest A&F University Animal Care and Experimental Ethics Committee.

Competing interests

The authors declare no competing interests.

Author details

[1]Department of Clinical Veterinary Medicine, College of Veterinary Medicine, Northwest A&F University, Yangling 712100, Shaanxi, China. [2]Key Laboratory of Animal Biotechnology of the Ministry of Agriculture and Rural Affairs, College of Veterinary Medicine, Northwest A&F University, Yangling 712100, Shaanxi, China. [3]Department of Preventive Veterinary Medicine, College of Veterinary Medicine, Northwest A&F University, Yangling 712100, Shaanxi, China.

Received: 22 November 2024 Accepted: 16 January 2025
Published online: 10 February 2025

References

1. Amin YA, Abdelaziz SG, Said AH. Treatment of postpartum endometritis induced by multidrug-resistant bacterial infection in dairy cattle by green

synthesized zinc oxide nanoparticles and in vivo evaluation of its broad spectrum antimicrobial activity in cow uteri. Res Vet Sci. 2023;165:105074.
2. Silva JCC, Siqueira LC, Rodrigues MX, Zinicola M, Wolkmer P, Pomeroy B, Bicalho RC. Intrauterine infusion of a pathogenic bacterial cocktail is associated with the development of clinical metritis in postpartum multiparous Holstein cows. J Dairy Sci. 2023;106:607–23.
3. Crookenden MA, Lake AVR, Burke CR, Pratt JT, Mitchell MD, Phyn CVC, Roche JR, Heiser A. Effect of nonsteroidal anti-inflammatory drugs on the inflammatory response of bovine endometrial epithelial cells in vitro. J Dairy Sci. 2023;106:2651–66.
4. Gärtner MA, Peter S, Jung M, Drillich M, Einspanier R, Gabler C. Increased mRNA expression of selected pro-inflammatory factors in inflamed bovine endometrium in vivo as well as in endometrial epithelial cells exposed to Bacillus pumilus in vitro. Reprod Fertil Dev. 2016;28:982–94.
5. Diaz-Lundahl S, Heringstad B, Garmo RT, Gillund P, Krogenæs AK. Heritability of subclinical endometritis in Norwegian Red cows. J Dairy Sci. 2022;105:5946–53.
6. Sheldon IM, Cronin JG, Pospiech M, Turner ML. Symposium review: Mechanisms linking metabolic stress with innate immunity in the endometrium. J Dairy Sci. 2018;101:3655–64.
7. Liu C, Tang X, Zhang W, Li G, Chen Y, Guo A, Hu C. 6-Bromoindirubin-3'-Oxime Suppresses LPS-Induced Inflammation via Inhibition of the TLR4/NF-κB and TLR4/MAPK Signaling Pathways. Inflammation. 2019;42:2192–204.
8. Kandikattu HK, Manohar M, Upparahalli Venkateshaiah S, Yadavalli C, Mishra A. Chronic inflammation promotes epithelial-mesenchymal transition-mediated malignant phenotypes and lung injury in experimentally-induced pancreatitis. Life Sci. 2021;278: 119640.
9. Youssef KK, Nieto MA. Epithelial-mesenchymal transition in tissue repair and degeneration. Nat Rev Mol Cell Biol. 2024;25:720–39.
10. Oghbaei F, Zarezadeh R, Jafari-Gharabaghlou D, Ranjbar M, Nouri M, Fattahi A, Imakawa K. Epithelial-mesenchymal transition process during embryo implantation. Cell Tissue Res. 2022;388:1–17.
11. López-Novoa JM, Nieto MA. Inflammation and EMT: an alliance towards organ fibrosis and cancer progression. EMBO Mol Med. 2009;1:303–14.
12. Peng L, Wen L, Shi Q-F, Gao F, Huang B, Meng J, Hu C-P, Wang C-M. Scutellarin ameliorates pulmonary fibrosis through inhibiting NF-κB/NLRP3-mediated epithelial-mesenchymal transition and inflammation. Cell Death Dis. 2020;11:978.
13. Xiao K, He W, Guan W, Hou F, Yan P, Xu J, Zhou T, Liu Y, Xie L. Mesenchymal stem cells reverse EMT process through blocking the activation of NF-κB and Hedgehog pathways in LPS-induced acute lung injury. Cell Death Dis. 2020;11:863.
14. Frakes AE, Dillin A. The UPRER: Sensor and Coordinator of Organismal Homeostasis. Mol Cell. 2017;66:761–71.
15. Liu Z, Nan P, Gong Y, Tian L, Zheng Y, Wu Z: Endoplasmic reticulum stress-triggered ferroptosis via the XBP1-Hrd1-Nrf2 pathway induces EMT progression in diabetic nephropathy. Biomedicine & Pharmacotherapy = Biomedecine & Pharmacotherapie 2023, 164:114897.
16. Gao L, Chen H, Li C, Xiao Y, Yang D, Zhang M, Zhou D, Liu W, Wang A, Jin Y. ER stress activation impairs the expression of circadian clock and clock-controlled genes in NIH3T3 cells via an ATF4-dependent mechanism. Cell Signal. 2019;57:89–101.
17. Xu G, Liu K, Anderson J, Patrene K, Lentzsch S, Roodman GD, Ouyang H. Expression of XBP1s in bone marrow stromal cells is critical for myeloma cell growth and osteoclast formation. Blood. 2012;119:4205–14.
18. Ferrè S, Deng Y, Huen SC, Lu CY, Scherer PE, Igarashi P, Moe OW. Renal tubular cell spliced X-box binding protein 1 (Xbp1s) has a unique role in sepsis-induced acute kidney injury and inflammation. Kidney Int. 2019;96:1359–73.
19. Liu L, Zhao M, Jin X, Ney G, Yang KB, Peng F, Cao J, Iwawaki T, Del Valle J, Chen X, Li Q. Adaptive endoplasmic reticulum stress signalling via IRE1α-XBP1 preserves self-renewal of haematopoietic and pre-leukaemic stem cells. Nat Cell Biol. 2019;21:328–37.
20. Bensellam M, Chan JY, Lee K, Joglekar MV, Hardikar AA, Loudovaris T, Thomas HE, Jonas J-C, Laybutt DR. Phlda3 regulates beta cell survival during stress. Sci Rep. 2019;9:12827.
21. Hassler JR, Scheuner DL, Wang S, Han J, Kodali VK, Li P, Nguyen J, George JS, Davis C, Wu SP, et al. The IRE1α/XBP1s Pathway Is Essential for the Glucose Response and Protection of β Cells. PLoS Biol. 2015;13:e1002277.
22. Shaffer AL, Shapiro-Shelef M, Iwakoshi NN, Lee A-H, Qian S-B, Zhao H, Yu X, Yang L, Tan BK, Rosenwald A, et al. XBP1, downstream of Blimp-1, expands the secretory apparatus and other organelles, and increases protein synthesis in plasma cell differentiation. Immunity. 2004;21:81–93.
23. Yang D, Jiang T, Liu J, Hong J, Lin P, Chen H, Zhou D, Tang K, Wang A, Jin Y. Hormone regulates endometrial function via cooperation of endoplasmic reticulum stress and mTOR-autophagy. J Cell Physiol. 2018;233:6644–59.
24. Xiao J, Liu S, Yu T, Zhang R, Guo X, Jia Y, Shang C, Wang A, Jin Y, Lin P: UFMylation is associated with LPS-induced inflammatory response in goat endometrial epithelial cells. Reproduction In Domestic Animals = Zuchthygiene 2020, 55:1725–1734.
25. Zhang X, Yu T, Guo X, Zhang R, Jia Y, Shang C, Wang A, Jin Y, Lin P. Ufmylation regulates granulosa cell apoptosis via ER stress but not oxidative stress during goat follicular atresia. Theriogenology. 2021;169:47–55.
26. Yi Y, Gao K, Zhang L, Lin P, Wang A, Jin Y. Zearalenone Induces MLKL-Dependent Necroptosis in Goat Endometrial Stromal Cells via the Calcium Overload/ROS Pathway. Int J Mol Sci. 2022;23:10170.
27. Zhang J, Zhao L, Li Y, Dong H, Zhang H, Zhang Y, Ma T, Yang L, Gao D, Wang X, et al. Circadian clock regulates granulosa cell autophagy through NR1D1-mediated inhibition of ATG5. Am J Physiol Cell Physiol. 2022;322:C231–45.
28. Gao K, Yi Y, Xue Z, Wang Z, Huang S, Zhang B, Lin P, Wang A, Chen H, Jin Y. Downregulation of XBP1s aggravates lipopolysaccharide-induced inflammation by promoting NF-κB and NLRP3 pathways' activation in goat endometrial epithelial cells. Theriogenology. 2023;210:119–32.
29. Duan J, Matute JD, Unger LW, Hanley T, Schnell A, Lin X, Krupka N, Griebel P, Lambden C, Sit B, et al. Endoplasmic reticulum stress in the intestinal epithelium initiates purine metabolite synthesis and promotes Th17 cell differentiation in the gut. Immunity. 2023;56:1115–31.
30. Jiang H, Ding D, He Y, Li X, Xu Y, Liu X: Xbp1s-Ddit3 promotes MCT-induced pulmonary hypertension. Clinical Science (London, England : 1979) 2021, 135:2467–2481.
31. Parasar P, Guru N, Nayak NR. Contribution of macrophages to fetomaternal immunological tolerance. Hum Immunol. 2021;82:325–31.
32. Druker SA, Sicsic R, van Straten M, Goshen T, Kedmi M, Raz T. Cytological endometritis diagnosis in primiparous versus multiparous dairy cows. J Dairy Sci. 2022;105:665–83.
33. Helfrich AL, Reichenbach H-D, Meyerholz MM, Schoon H-A, Arnold GJ, Fröhlich T, Weber F, Zerbe H. Novel sampling procedure to characterize bovine subclinical endometritis by uterine secretions and tissue. Theriogenology. 2020;141:186–96.
34. Bretzlaff K. Rationale for treatment of endometritis in the dairy cow. Vet Clin North Am Food Anim Pract. 1987;3:593–607.
35. Zhou Y, Huang X, Yu H, Shi H, Chen M, Song J, Tang W, Teng F, Li C, Yi L, et al. TMT-based quantitative proteomics revealed protective efficacy of Icariside II against airway inflammation and remodeling via inhibiting LAMP2, CTSD and CTSS expression in OVA-induced chronic asthma mice. Phytomedicine : International Journal of Phytotherapy and Phytopharmacology. 2023;118:154941.
36. He G, Ma M, Yang W, Wang H, Zhang Y, Gao M-Q. SDF-1 in Mammary Fibroblasts of Bovine with Mastitis Induces EMT and Inflammatory Response of Epithelial Cells. Int J Biol Sci. 2017;13:604–14.
37. Zhao C, Hu X, Qiu M, Bao L, Wu K, Meng X, Zhao Y, Feng L, Duan S, He Y, et al. Sialic acid exacerbates gut dysbiosis-associated mastitis through the microbiota-gut-mammary axis by fueling gut microbiota disruption. Microbiome. 2023;11:78.
38. Ni H, Ou Z, Wang Y, Liu Y, Sun K, Zhang J, Zhang J, Deng W, Zeng W, Xia R, et al. XBP1 modulates endoplasmic reticulum and mitochondria crosstalk via regulating NLRP3 in renal ischemia/reperfusion injury. Cell Death Discovery. 2023;9:69.
39. Liao J, Hu Z, Li Q, Li H, Chen W, Huo H, Han Q, Zhang H, Guo J, Hu L, et al. Endoplasmic Reticulum Stress Contributes to Copper-Induced Pyroptosis via Regulating the IRE1α-XBP1 Pathway in Pig Jejunal Epithelial Cells. J Agric Food Chem. 2022;70:1293–303.
40. Zhang Z, Qian Q, Li M, Shao F, Ding W-X, Lira VA, Chen SX, Sebag SC, Hotamisligil GS, Cao H, Yang L. The unfolded protein response regulates hepatic autophagy by sXBP1-mediated activation of TFEB. Autophagy. 2021;17:1841–55.
41. Zhang S, Tang J, Sun C, Zhang N, Ning X, Li X, Wang J. Dexmedetomidine attenuates hepatic ischemia-reperfusion injury-induced apoptosis via

reducing oxidative stress and endoplasmic reticulum stress. Int Immunopharmacol. 2023;117:109959.
42. Acosta-Alvear D, Zhou Y, Blais A, Tsikitis M, Lents NH, Arias C, Lennon CJ, Kluger Y, Dynlacht BD. XBP1 controls diverse cell type- and condition-specific transcriptional regulatory networks. Mol Cell. 2007;27:53–66.
43. Wen M, Ma X, Cheng H, Jiang W, Xu X, Zhang Y, Zhang Y, Guo Z, Yu Y, Xu H, et al. Stk38 protein kinase preferentially inhibits TLR9-activated inflammatory responses by promoting MEKK2 ubiquitination in macrophages. Nat Commun. 2015;6:7167.
44. Ashton KJ, Reichelt ME, Mustafa SJ, Teng B, Ledent C, Delbridge LMD, Hofmann PA, Morrison RR, Headrick JP. Transcriptomic effects of adenosine 2A receptor deletion in healthy and endotoxemic murine myocardium. Purinergic Signalling. 2017;13:27–49.
45. Kesavan K, Lobel-Rice K, Sun W, Lapadat R, Webb S, Johnson GL, Garrington TP. MEKK2 regulates the coordinate activation of ERK5 and JNK in response to FGF-2 in fibroblasts. J Cell Physiol. 2004;199:140–8.

Publisher's Note